

Design of network-coding based multi-edge type LDPC codes for a multi-source relaying system

Jun Li, Marwan H. Azmi, Robert Malaney, and Jinhong Yuan

School of Electrical Engineering and Telecommunications,
University of New South Wales, Sydney, NSW 2052, AUSTRALIA

Email: jun.li@unsw.edu.au, marwan@student.unsw.edu.au, r.malaney@unsw.edu.au, j.yuan@unsw.edu.au

Abstract—In this paper we investigate a multi-source LDPC coding scheme for a Gaussian relay system, where M sources communicate with the destination under the help of a single relay ($M-1-1$ system). More specifically, we propose a network coded LDPC coding scheme for the $M-1-1$ system where network coding over all sources' data is performed at the relay. A challenge in such a scheme is the code design for asymmetric channels where each source has different code rate. To address this issue, we present here a novel scheme named network coded multi-edge type LDPC code (NCMET-LDPC). Within NCMET-LDPC we optimize the code profiles by EXIT charts, and show that our coding scheme achieves better bit error rate (BER) performance relative to existing schemes.

I. INTRODUCTION

Low-density parity-check (LDPC) codes have been shown to approach theoretical capacity limits for single link communication channels [1]. Recently, distributed LDPC for cooperative communications has attracted much attention. The work of [2] first explored the use of bilayer LDPC codes within the cooperative single source channel ($1-1-1$ system) with a full-duplexing relay. In [3], multi-edge type LDPC code [4] was utilized to design the bilayer LDPC codes. Codes designed in this manner we refer to as BMET-LDPC codes. The work of [5] considered more practical issues (e.g. Rayleigh fading channels and the half-duplexing relay) in the $1-1-1$ system.

However, the above studies on distributed LDPC codes are all limited to the one-source scenario. In this paper, we investigate LDPC code design for a cooperative system with multi-source and one relay ($M-1-1$ system). Based on existing methods of distributed LDPC code design (e.g. BMET-LDPC codes) in the $1-1-1$ system, an intuitive thought is that the relay serves the sources in a round-robin fashion, optimizing the BMET-LDPC codes for a single source in each round. Unfortunately, such a direct application may lose any potential benefit of joint processing at the relay.

In this paper, we design LDPC codes where joint processing at the relay is in the form of network coding [6]. We notice that [7] proposes a network coded bilayer LDPC coding scheme in the $M-1-1$ system. However, it only considers a very special case where all source-to-relay channels have the same achievable rate, and all source-to-destination channels have the same achievable rate. Here, we propose a novel code scheme, *i.e.*, the NCMET-LDPC code for the $M-1-1$ model to address the more general case where each channel has

different achievable rate. Within this scheme an EXIT chart analysis is utilized to optimize the code profiles.

II. SYSTEM MODEL AND PRELIMINARIES

Fig. 1(a) shows a Gaussian relay system with M sources, 1 relay and 1 destination, where sources s_1, \dots, s_M transmit information to the destination d simultaneously. In this figure the full-duplex relay r receives the signals and implements with the decode-and-forward protocol. Suppose that the m -th source, s_m , transmits its information in the frequency band f_m , and the relay r has M parts r_1, \dots, r_M receiving and transmitting at f_1, \dots, f_M , respectively. In this scenario the multi-source system can be viewed as M independent parallel $1-1-1$ systems.

Without loss of generality, let us consider the m -th source, s_m and its corresponding $1-1-1$ system composed of s_m, r_m and d , where r_m is the part of the relay r operating at f_m . Suppose X_m is the signal transmitted by s_m , which has the average power P_m , and X_{1m} is the signal transmitted by r_m , which has the average power P_{1m} . The noises at r_m and d are Gaussian distributed with power N_{1m} and $N_{1m} + N_{2m}$, respectively. The binning scheme [2] is used to obtain the achievable rate of the $1-1-1$ system. In this binning scheme, s_m divides its total power P_m into a fraction αP_m for the i -th codeword ω_i , and a fraction $(1-\alpha)P_m$ for the bin index ϕ_i of the previous $(i-1)$ -th codeword ω_{i-1} . Since r_m has successfully decoded ω_{i-1} in the previous time slot, ω_i can be decoded successfully at r_m with rate

$$R_+^m \leq \frac{1}{2} \log \left(1 + \frac{\alpha P_m}{N_{1m}} \right). \quad (1)$$

Meanwhile, r_m is transmitting $X_{1m}(\phi_i)$ to d . Thus, d receives the interferential signal composed by X_m and X_{1m} in the frequency band f_m . By successive interference cancellation, d firstly treats X_m as noise so as to extract the bin index ϕ_i with a rate no more than

$$R_1^m = \frac{1}{2} \log \left(1 + \frac{(\sqrt{P_{1m}} + \sqrt{(1-\alpha)P_m})^2}{\alpha P_m + N_{1m} + N_{2m}} \right). \quad (2)$$

Then combining with ϕ_i , the decoding of ω_{i-1} at d will be successful with a rate no more than

$$R_-^m = \frac{1}{2} \log \left(1 + \frac{\alpha P_m}{N_{1m} + N_{2m}} \right). \quad (3)$$

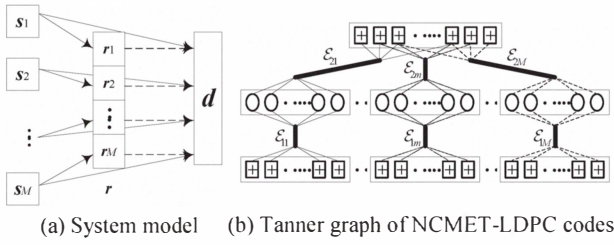


Fig. 1. System model and the Tanner graph of NCMET-LDPC codes.

From the above three equations, we obtain the overall rate for the Gaussian relay channel (operating in f_m) as $R_m = \max \min \{R_+^m, R_1^m + R_-^m\}$. To maximize R_m , we let $R_+^m = R_1^m + R_-^m$ by adapting α .

BMET-LDPC codes can be utilized to approach the rates R_+^m and R_-^m in the m -th $1-1-1$ system [3]. So in the $M-1-1$ case, a code design technique could be the use of BMET-LDPC individually to each source. However, in such technique the relay only produces the parity check digits for each source based on its own messages. Since the relay has the knowledge of all the sources' data, the network coded parity check bits, which are produced by the relay by jointly combining the digits from all the sources, connect all the sources' frames as a code block. Thus the code length is increased and higher coding gain can be achieved. Based on this we now propose a novel code scheme, *i.e.* the NCMET-LDPC code for the $M-1-1$ system.

III. NETWORK CODED MULTI-EDGE TYPE LDPC CODES

The structure of an NCMET-LDPC code is shown in Fig. 1(b). The check nodes in the upper graph correspond to the network coded digits generated by the relay. To accommodate the case where the achievable rates for all the source-to-relay channels (or all the source-to-destination channels) are different (asymmetric channels), we introduce multi-edge types and represent the different edge types as \mathcal{E} with different subscripts as shown in Fig. 1. Similar to BMET-LDPC code design, we assume that all the source-to-relay links and relay-to-destination links are error-free.

The multi-edge type LDPC code design for an $M-1-1$ system begins with the optimization of the lower Tanner graph at rates R_+^1, \dots, R_+^M for s_1, \dots, s_M , respectively. Following the same notations of [4], the m -th lower sub-graph ensemble of the multi-edge type LDPC codes for s_m is

$$v_m(\mathbf{r}, \mathbf{x}) = r_1 \sum_{d_{1m}=1}^{d_{v1,m}} v_{[0,1],[d_{1m}]} x_{1m}^{d_{1m}}, \quad (4)$$

$$\mu_m(\mathbf{x}) = \sum_{d_{1m}=1}^{d_{c1,m}} \mu_{[d_{1m}]} x_{1m}^{d_{1m}},$$

where $[0, 1]$ is the vector \mathbf{b} and $[d_{1m}]$ is the vector \mathbf{d} in [4]. Vector $\mathbf{b} = [0, 1]$ means that all variable nodes related to the digits of s_m are transmitted through the $s_m \rightarrow r_m$ channel ($b_1 = 1$) at rate R_+^m , and there are no punctured variables

($b_0 = 0$) in the codeword of the m -th lower sub-graph. Vector \mathbf{d} contains only one element since there is only one edge type. The variable d_{1m} represents the degree of variable nodes belonging to s_m , with a maximum value $d_{v1,m}$. The variable d_{1m} also represents the degree of check nodes belonging to s_m , with a maximum value $d_{c1,m}$. Since all the blocks transmitted by s_m and r_m have the same length n , the quantity $v_{\mathbf{b},\mathbf{d}} n$ is the number of variable nodes of type (\mathbf{b}, \mathbf{d}) and $\mu_{\mathbf{d}} n$ is the number of check nodes of the type (\mathbf{d}) in the lower sub-graph. The code rate of the m -th lower sub-graph for s_m is $R_+^m = 1 - \sum_{d_{1m}=1}^{d_{c1,m}} \mu_{[d_{1m}]}$.

Also shown in Fig. 1(b) is the network coding at the relay. The relay transmits the network coded parity check digits to the destination bounded by the total rate $R_1 = \sum_{m=1}^M R_m^1$. Note that, nR_m^1 are the effective digits allocated to s_m . We can view the whole Tanner graph as M $1-1-1$ independent systems (sub-graphs). The m -th sub-graph for s_m contains the edge type \mathcal{E}_{1m} , and the edge type \mathcal{E}_{2m} . As such, the polynomials for the m -th sub-graph can be written as

$$v_m(\mathbf{r}, \mathbf{x}) = r_1 \sum_{d_{1m}=1}^{d_{v1,m}} \sum_{d_{2m}=0}^{d_{v2,m}} v_{[0,1],[d_{1m},d_{2m}]} x_{1m}^{d_{1m}} x_{2m}^{d_{2m}}, \quad (5)$$

$$\mu_m(\mathbf{x}) = \sum_{d_{1m}=1}^{d_{c1,m}} \mu_{[d_{1m},0]} x_{1m}^{d_{1m}} + \sum_{d_{2m}=1}^{d_{c2,m}} \mu_{[0,d_{2m}]} x_{2m}^{d_{2m}}.$$

Note that now $\mathbf{d} = [d_{1m}, d_{2m}]$ in (5) represents two edge types. Here, d_{1m} and d_{2m} denote the variable node degree (or the check node degree) of the two edge types \mathcal{E}_{1m} and \mathcal{E}_{2m} , respectively. The maximum degree \mathcal{E}_{km} , ($k = 1, 2$) connected to a variable node and a check node are $d_{vk,m}$ and $d_{ck,m}$, respectively.

We now introduce another polynomial associated to the check nodes in the upper part of the Tanner graph (the upper graph), namely,

$$\mu(\mathbf{x}) = \sum_{d_{21}=0}^{d_{c2,1}} \cdots \sum_{d_{2M}=0}^{d_{c2,M}} \mu_{[d_{21}, \dots, d_{2M}]} x_{21}^{d_{21}} \cdots x_{2M}^{d_{2M}}, \quad (6)$$

where now the vector $\mathbf{d} = [d_{21}, \dots, d_{2M}]$ represents M edge types connected to the check nodes in the upper graph. We denote d_{21}, \dots, d_{2M} as the degree of $\mathcal{E}_{21}, \dots, \mathcal{E}_{2M}$ that are connected to a check node in the upper graph, respectively. Note that there is a relationship between $\mu_{[d_{21}, \dots, d_{2M}]}$ in (6) and $\mu_{[0,d_{2m}]}$ for the m -th sub-graph in (5) as

$$\mu_{[0,d_{2m}]} = \sum_{\sim d_{2m}} \mu_{[d_{21}, \dots, d_{2M}]}, \quad \text{and}$$

$$\sum_{\sim d_{2m}} = \sum_{d_{21}=0}^{d_{c2,1}} \cdots \sum_{d_{2(m-1)}=0}^{d_{c2,m-1}} \sum_{d_{2(m+1)}=0}^{d_{c2,m+1}} \cdots \sum_{d_{2M}=0}^{d_{c2,M}}. \quad (7)$$

The code structure in the m -th sub-graph should satisfy

$$\begin{aligned} R_-^m &= 1 - \sum_{d_{1m}=1}^{d_{c1,m}} \mu_{[d_{1m},0]} - R_1^m, \\ R_1^m &= \sum_{d_{2m}=1}^{d_{c2,m}} \sum_{\sim d_{2m}} \frac{\mu_{[d_{21},\dots,d_{2M}]d_{2m}}}{\sum_{l=1}^M d_{2l}}, \end{aligned} \quad (8)$$

where R_1^m is determined according to [8]. We optimize the whole system by treating the blocks of all the sources as a super block. Besides (8), there are some other constraints that should be satisfied. Firstly, there are constraints between the variable nodes and the check nodes for each of the M sub-graphs. Secondly, there are constraints between the variable nodes and the check nodes for the lower part of each sub-graph (lower sub-graph). These constraints can be written

$$\begin{aligned} \sum_{d_{2m}=1}^{d_{c2,m}} \mu_{[0,d_{2m}]} d_{2m} &= \sum_{d_{1m}=1}^{d_{v1,m}} \sum_{d_{2m}=0}^{d_{v2,m}} v_{[0,1],[d_{1m},d_{2m}]} d_{2m}, \\ \sum_{d_{1m}=1}^{d_{c1,m}} \mu_{[d_{1m}]} d_{1m} &= \sum_{d_{1m}=1}^{d_{v1,m}} v_{[0,1],[d_{1m}]} d_{1m}. \end{aligned} \quad (9)$$

Other constraints are the relationships between the m -th lower sub-graph and the m -th sub-graph, *i.e.* $\mu_{[d_{1m}]} = \mu_{[d_{1m},0]}$ and $v_{[0,1],[d_{1m}]} = \sum_{d_{2m}=0}^{d_{v2,m}} v_{[0,1],[d_{1m},d_{2m}]}$.

Let us now define some parameters which will be used in the EXIT analysis in the next section. Firstly, we define $\lambda_{[d_{1m},d_{2m}]}^{km}$, $k = 1, 2$, as the percentage of the edges in the type \mathcal{E}_{km} , which are connected to the variable nodes with d_{1m} edges of the type \mathcal{E}_{1m} and d_{2m} edges of the type \mathcal{E}_{2m} . This can be written,

$$\lambda_{[d_{1m},d_{2m}]}^{km} = \frac{v_{[0,1],[d_{1m},d_{2m}]} d_{km}}{\sum_{d_{1l}=1}^{d_{v1,m}} \sum_{d_{2l}=0}^{d_{v2,m}} v_{[0,1],[d_{1l},d_{2l}]} d_{kl}}. \quad (10)$$

We define $\lambda_{[d_{1m},d_{2m}]}^m$ as the percentage of the edges in either the type \mathcal{E}_{1m} or the type \mathcal{E}_{2m} , which are connected to the variable nodes with d_{1m} edges of the type \mathcal{E}_{1m} and d_{2m} edges of the type \mathcal{E}_{2m} . This can be written,

$$\lambda_{[d_{1m},d_{2m}]}^m = \frac{v_{[0,1],[d_{1m},d_{2m}]} (d_{1m} + d_{2m})}{\sum_{d_{1l}=1}^{d_{v1,m}} \sum_{d_{2l}=0}^{d_{v2,m}} v_{[0,1],[d_{1l},d_{2l}]} (d_{1l} + d_{2l})}. \quad (11)$$

We also define $\rho_{[d_{1m}]}^{1m}$ as the percentage of the edges in the type \mathcal{E}_{1m} , which are connected to the check nodes in the m -th lower sub-graph with d_{1m} edges of type \mathcal{E}_{1m} . This can be written,

$$\rho_{[d_{1m}]}^{1m} = \frac{\mu_{[d_{1m}]} d_{1m}}{\sum_{d_{1l}=1}^{d_{c1,m}} \mu_{[d_{1l}]} d_{1l}}. \quad (12)$$

Finally, we define $\rho_{[d_{21},\dots,d_{2M}]}^{2m}$ as the percentage of the edges in the type \mathcal{E}_{2m} , which are connected to the check nodes in the upper graph with d_{2m} edges of type \mathcal{E}_{2m} . This can be written,

$$\rho_{[d_{21},\dots,d_{2M}]}^{2m} = \frac{\mu_{[d_{21},\dots,d_{2M}]d_{2m}}}{\sum_{d_{2l}=0}^{d_{c2,m}} \mu_{[0,d_{2l}]} d_{2l}}. \quad (13)$$

IV. EXIT ANALYSIS AND CODES PROFILE OPTIMIZATION

The utilization of the EXIT analysis that characterizes the amplification of extrinsic mutual information (EMI) between the input and the output of the decoder at the destination, significantly facilitates the analysis of iterative coding schemes, and improves the code search process.

A. EMI Propagation Model

Since, in our system model, the codeword digits of different sources experience different channel conditions, we average the EMI in each edge type. We denote the variable nodes set associated with the codeword digits of s_m as V_m , the check nodes set associated with the parity check digits of s_m in the m -th lower sub-graph as C_{1m} , and the shared check nodes set associated with the network coded parity check digits of the relay in the upper graph as C_2 . The mutual information of the $s_m \rightarrow d$ channel is denoted by I_{ch}^m . Since V_m is connected to two edge types, *i.e.* \mathcal{E}_{1m} and \mathcal{E}_{2m} , we define four kinds of EMI as follows [10].

1. I_{Ev}^{1m} : The EMI between the message sent from V_m to C_{1m} and the associated codeword digit, on each edge in the type \mathcal{E}_{1m} connecting V_m to C_{1m} ;
2. I_{Ev}^{2m} : The EMI between the message sent from V_m to C_2 and the associated codeword digit, on each edge in the type \mathcal{E}_{2m} connecting V_m to C_2 ;
3. I_{Ec}^{1m} : The EMI between the message sent from C_{1m} to V_m and the associated codeword digit, on each edge in the edge type \mathcal{E}_{1m} connecting C_{1m} to V_m ;
4. I_{Ec}^{2m} : The EMI between the message sent from C_2 to V_m and the associated codeword digit, on each edge in the edge type \mathcal{E}_{2m} connecting C_2 to V_m .

Also note that the EMI on an edge connecting V_m to C_{1m} (or C_2), at the output of the variable node, is the *a priori* mutual information (AMI) for C_{1m} (or C_2), *i.e.* $I_{Ev}^{1m} = I_{Ac}^{1m}$ (or $I_{Ev}^{2m} = I_{Ac}^{2m}$). Similarly, the EMI on an edge connecting C_{1m} (or C_2) to V_m , at the output of the check node, is the AMI for V_m , *i.e.* $I_{Ec}^{1m} = I_{Av}^{1m}$ (or $I_{Ec}^{2m} = I_{Av}^{2m}$).

B. EXIT Analysis for NCMET-LDPC

The EXIT functions for variable nodes and check nodes on the AWGN channel have been introduced in [9]. For the signals transmitted by s_m , we define $(1/\sigma_m)^2$ as its received signal-to-noise ratio (SNR) at the destination. For the log-likelihood ratio (LLR) message of the $s_m \rightarrow d$ channel, we denote its variance as $(\sigma_{ch}^m)^2$. Note that, $\sigma_{ch}^m = 2/\sigma_m$. Since each source transmits the BPSK symbols, we use $J(\sigma_{ch}^m)$ to represent the capacity of a binary input additive Gaussian noise channel, which is given by [9]

$$J(\sigma_{ch}^m) = 1 - \int_{-\infty}^{+\infty} \frac{e^{-(\xi - (\sigma_{ch}^m)^2/2)^2 / 2(\sigma_{ch}^m)^2}}{\sqrt{2\pi\sigma_{ch}^m}} \cdot \log_2(1 + e^{-\xi}) d\xi \quad (14)$$

where the integral variable ξ represents the LLR value of the channel. Then we have the iterative four-step process as follows.

1. Initialization

We initialize that $I_{ch}^m = J(\sigma_{ch}^m)$, for $m = 1, \dots, M$.

2. Variable nodes to check nodes update

For $m = 1, \dots, M$, $k = 1, 2$, and $\bar{k} = 3 - k$, we have

$$I_{Ev}^{km} = \sum_{d_{km}=1}^{d_{vk,m}} \sum_{d_{\bar{k}m}=0}^{d_{v\bar{k},m}} J\left(\sqrt{\varphi_V^{km}}\right) \lambda_{[d_{km}, d_{\bar{k}m}]}^{km}, \quad (15)$$

where

$$\varphi_V^{km} = (d_{km} - 1) \left(J^{-1}\left(I_{Av}^{km}\right)\right)^2 + d_{\bar{k}m} \left(J^{-1}\left(I_{A\bar{v}}^{\bar{k}m}\right)\right)^2 + \left(J^{-1}\left(I_{ch}^m\right)\right)^2. \quad (16)$$

3. Check nodes to variable nodes update

The update from check nodes to variable nodes is more complicated. To obtain the more accurate EMI value generated by the check nodes, we follow the method in [11]. We define the function $F_j(\sigma)$ as follows.

$$F_j(\sigma) = \int_{-1}^{+1} \frac{2\zeta^{2j}}{(1-\zeta^2)\sqrt{2\pi}\sigma} e^{-\frac{(\ln \frac{1+\zeta}{1-\zeta} - \frac{\sigma^2}{2})^2}{2\sigma^2}} d\zeta, \quad (17)$$

where the integral variable ζ represents the ‘‘soft bit’’. Note that $\zeta = \tanh((\xi_\zeta)/2)$, where ξ_ζ is the LLR value corresponding to ζ . The EMI on an edge type \mathcal{E}_{1m} connecting C_{1m} to V_m , at the output of the check node is

$$I_{Ec}^{1m} = \frac{1}{\ln 2} \sum_{d_{1m}=1}^{d_{c1,m}} \sum_{j=1}^{\infty} \frac{\left(F_j\left(J^{-1}\left(I_{Ac}^{1m}\right)\right)\right)^{d_{1m}-1}}{2j(2j-1)} \rho_{[d_{1m}]}^{1m}. \quad (18)$$

The extrinsic mutual information (EMI) on an edge type \mathcal{E}_{2m} connecting C_2 to V_m at the output of the check node is more complicated since more than one source participates in the generation of C_2 . We have

$$I_{Ec}^{2m} = \frac{1}{\ln 2} \sum_{d_{2m}=1}^{d_{c2,m}} \sum_{\sim d_{2m}} \sum_{j=1}^{\infty} \frac{\rho_{[d_{21}, \dots, d_{2M}]}^{2m}}{2j(2j-1)} \left(F_j\left(J^{-1}\left(I_{Ac}^{2m}\right)\right)\right)^{d_{2m}-1} \prod_{\substack{m'=1 \\ m' \neq m}}^M \left(F_j\left(J^{-1}\left(I_{Ac}^{2m'}\right)\right)\right)^{d_{2m'}}. \quad (19)$$

After the update from check nodes to variable nodes, go back to step 2 and begin the next round iteration. In each iteration process, we make $I_{Av}^{km} = I_{Ec}^{km}$ and $I_{Ac}^{km} = I_{Ev}^{km}$ for $k = 1, 2$. At the end of all the iterations, go to step 4.

4. Output and decision

Determine mutual information of the m -th source, I_m , via

$$I_V^m = \sum_{d_{1m}=1}^{d_{v1,m}} \sum_{d_{2m}=0}^{d_{v2,m}} \lambda_{[d_{1m}, d_{2m}]}^m J\left(\sqrt{\varphi_V^m}\right), \quad (20)$$

where

$$\varphi_V^m = d_{1m} \left(J^{-1}\left(I_{Av}^{1m}\right)\right)^2 + d_{2m} \left(J^{-1}\left(I_{Av}^{2m}\right)\right)^2 + \left(J^{-1}\left(I_{ch}^m\right)\right)^2. \quad (21)$$

A successful decoding is based on whether I_V^m approaches to 1 for $m = 1, \dots, M$.

C. Code Design and Optimization

We firstly fix the lower graph codes of all sources, choosing the optimal point-to-point LDPC code to approach capacity R_+^m . Then we optimize the overall Tanner graph to approach the achievable rate of the whole system. The code optimization involves finding the optimal degree distributions of the variable nodes related to the digits of each source, *i.e.* $v_{[0,1],[d_{1m}, d_{2m}]}$ for s_m , and the optimal check node degree distribution $\mu_{[d_{21}, \dots, d_{2M}]}$. The optimization problem is to maximize the system threshold, which is calculated as follows. Since the channel mutual information of the $s_m \rightarrow d$ channel is $J\left(\frac{2}{\sigma_m}\right)$, and all the sources are assumed to have the same block length, we compute the system mutual information as the average of the channel mutual information of all the sources. We can therefore write the system threshold as

$$\sigma_{sys} = \frac{2}{J^{-1}\left(\frac{1}{M} \sum_{m=1}^M J\left(\frac{2}{\sigma_m}\right)\right)}. \quad (22)$$

Then the optimization problem is formulated as,

$$\begin{aligned} & \text{maximize } \sigma_{sys} \\ & \text{subject to } I_V^m \rightarrow 1, \text{ for } m = 1, \dots, M. \end{aligned} \quad (23)$$

V. NUMERICAL RESULTS

Suppose all the sources transmit the BPSK signals and all the frames have the same length $n = 10^4$. We choose a 2-source case to illustrate the code design. The first source has the following rates: $R_+^1 = 0.7$, $R_-^1 = 0.5$ and $R_1^1 = 0.2$. The second source has the following rates: $R_+^2 = 0.58$, $R_-^2 = 0.38$ and $R_1^2 = 0.2$. Applying the proposed method, we get a code profile as shown in Table I.

We determine the distributions of \mathcal{E}_{11} and \mathcal{E}_{12} in the lower graphs for s_1 and s_2 to approach the rates R_+^1 and R_+^2 , respectively. These distributions can be directly obtained from [12]. Our main task is to find out the optimal distribution of \mathcal{E}_{21} and \mathcal{E}_{22} , and the corresponding $v_{[0,1],[d_{1,1}, d_{2,1}]}$, $v_{[0,1],[d_{1,2}, d_{2,2}]}$ and $\mu_{[0, d_{2,1}, d_{2,2}]}$.

By the searching criterion of (23) and EXIT curves fitting, we obtain the variable node distributions of the two sources, $v_{[0,1],[d_{1,1}, d_{2,1}]}$, $v_{[0,1],[d_{1,2}, d_{2,2}]}$, and the corresponding degrees shown in Table I. The check node distribution in the upper graph at the relay is $\mu_{[d_{1,m}, d_{2,m}]} = R_1^1 + R_1^2 = 0.4$. Each check node of the relay has the degree 6, among which, 3 edges are allocated to s_1 and the other 3 edges are allocated to s_2 . This is reasonable since $R_1^1 = R_1^2 = 0.2$. Note that the gap between the Shannon limits for the two rates, *i.e.* $R_-^1 = 0.5$ and $R_-^2 = 0.38$ is about 1.65 dB. Therefore, when searching the code, we set the gap between the two thresholds σ_1 and σ_2 according to their Shannon limit gap, and we obtain the two thresholds as $\sigma_1 = 0.9616$ and $\sigma_2 = 1.1561$.

We refer the NCMET-LDPC code in Table I as CODE-A. For comparison, we design the BMET-LDPC code for each source individually. By the same EXIT chart searching method, we obtain two profiles of BMET-LDPC codes. One is for the first source with $R_+^1 = 0.7$, $R_-^1 = 0.5$, $R_1^1 = 0.2$,

| Source 1 | | | Source 2 | | |
|---|--------------------|--------------------|----------------------------|--------------------|--------------------|
| Variable Node Distribution | | | | | |
| $v_{[0,1][d_{11},d_{21}]}$ | \mathcal{E}_{11} | \mathcal{E}_{21} | $v_{[0,1][d_{12},d_{22}]}$ | \mathcal{E}_{12} | \mathcal{E}_{22} |
| 0.244225 | 2 | 0 | 0.3289203 | 2 | 0 |
| 0.1531552 | 2 | 1 | 0.0772109 | 2 | 1 |
| 0.0209422 | 2 | 7 | 0.0531292 | 2 | 2 |
| 0.1930021 | 3 | 0 | 0.145309 | 3 | 0 |
| 0.138759 | 3 | 3 | 0.0149215 | 3 | 1 |
| 0.058304 | 6 | 0 | 0.123802 | 3 | 2 |
| 0.0109062 | 6 | 7 | 0.0286741 | 3 | 14 |
| 0.000131148 | 6 | 21 | 0.0346943 | 6 | 0 |
| 0.05680712 | 7 | 0 | 0.0101216 | 6 | 2 |
| 0.047728 | 7 | 2 | 0.092595 | 7 | 0 |
| 0.0556525 | 20 | 3 | 0.0297043 | 7 | 7 |
| 0.0203505 | 20 | 7 | 0.0165257 | 20 | 0 |
| | | | 0.00437642 | 20 | 1 |
| | | | 0.0400163 | 20 | 3 |
| Check Node Distribution in Lower Graph | | | | | |
| $\mu_{[d_{11},0]}$ | | \mathcal{E}_{11} | $\mu_{[d_{12},0]}$ | | \mathcal{E}_{12} |
| 0.3 | | 15 | 0.42 | | 10 |
| Check Node Distribution in Upper Graph | | | | | |
| $\mu_{[d_{21},d_{22}]}$ | | \mathcal{E}_{21} | $\mu_{[d_{21},d_{22}]}$ | | \mathcal{E}_{22} |
| 0.4×0.5 | | 3 | 0.4×0.5 | | 3 |

TABLE I

THE NODE DISTRIBUTION OF THE NCMET-LDPC IN TWO-SOURCE CASE.

| Source 1 | | | Source 2 | | |
|---|--------------------|--------------------|----------------------------|--------------------|--------------------|
| Variable Node Distribution | | | | | |
| $v_{[0,1][d_{11},d_{21}]}$ | \mathcal{E}_{11} | \mathcal{E}_{21} | $v_{[0,1][d_{12},d_{22}]}$ | \mathcal{E}_{12} | \mathcal{E}_{22} |
| 0.247137 | 2 | 0 | 0.343893 | 2 | 0 |
| 0.143731 | 2 | 1 | 0.115366 | 2 | 1 |
| 0.027432 | 2 | 6 | 0.17937 | 3 | 0 |
| 0.191186 | 3 | 0 | 0.13334 | 3 | 1 |
| 0.135883 | 3 | 1 | 0.0158 | 6 | 3 |
| 0.004730 | 3 | 3 | 0.02901 | 6 | 11 |
| 0.025454 | 6 | 3 | 0.1223 | 7 | 2 |
| 0.043946 | 6 | 9 | 0.0314072 | 20 | 1 |
| 0.071606 | 7 | 1 | 0.029511 | 20 | 4 |
| 0.032894 | 7 | 2 | | | |
| 0.039999 | 20 | 2 | | | |
| 0.036001 | 20 | 7 | | | |
| Check Node Distribution in Lower Graph | | | | | |
| $\mu_{[d_{11},0]}$ | | \mathcal{E}_{11} | $\mu_{[d_{12},0]}$ | | \mathcal{E}_{12} |
| 0.3 | | 15 | 0.42 | | 10 |
| Check Node Distribution in Upper Graph | | | | | |
| $\mu_{[0,d_{21}]}$ | | \mathcal{E}_{21} | $\mu_{[0,d_{22}]}$ | | \mathcal{E}_{22} |
| 0.082626 | | 6 | 0.1907 | | 5 |
| 0.117374 | | 7 | 0.0093 | | 6 |

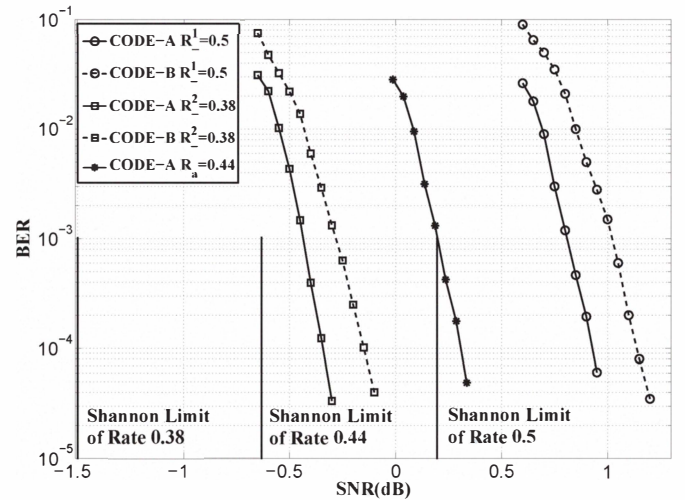
TABLE II

THE NODE DISTRIBUTION OF THE BMET-LDPC FOR EACH SOURCE.

and one is for the second source with $R_+^2 = 0.58$, $R_-^2 = 0.38$, $R_1^2 = 0.2$. The BMET-LDPC codes are shown in Table II, both of which we refer to as CODE-B. Fig. 2 shows the BER curves for CODE-A and CODE-B. In terms of BER performance, we can see CODE-A performs better than CODE-B.

VI. CONCLUSION

In this paper, we have investigated a new code design (NCMET-LDPC) for a multi-source relaying system. We have proposed a code structure of the asymmetric channels where


 Fig. 2. BER curves for NCMET-LDPC code (CODE-A) and BMET-LDPC code (CODE-B). The super block has the rate $R_a = 0.44$.

the achievable rates for all the source-to-relay channels (or all the source-to-destination channels) are different. We have shown that our new scheme delivers better BER performance compared to the traditional schemes that do not use network coding at the relay.

This work has been supported by the Australian Research Council under ARC Grant DP087940.

REFERENCES

- [1] T. J. Richardson, M. A. Shokrollahi, and R. L. Urbanke, "Design of capacity-approaching irregular low-density parity-check codes," *IEEE Trans. Inf. Theory*, vol. 47, no. 2, pp. 619-637, Feb. 2001.
- [2] P. Razaghi and W. Yu, "Bilayer low-density parity-check codes for decode-and-forward in relay channels," *IEEE Trans. Inf. Theory*, vol. 53, no. 10, pp. 3723-3739, Oct. 2007.
- [3] M. H. Azmi and J. Yuan, "Design of multi-edge type bilayer-expurgated LDPC codes," *IEEE International Symposium on Information Theory (ISIT)*, pp. 1988-1992, Jun. 2009.
- [4] T. J. Richardson and R. L. Urbanke, "Multi-edge type LDPC codes," Available Online: <http://lthcwww.epfl.ch/papers/multiedge.ps>.
- [5] A. Chakrabarti, A. de Baynast, A. Sabharwal, and B. Aazhang, "Low density parity check codes for the relay channel," *IEEE J. of Sel. Areas Commun.*, vol. 25, pp. 280-291, Feb. 2007.
- [6] R. Ahlswede, N. Cai, S.-Y. R. Li and R. W. Yeung, "Network information flow," *IEEE Trans. Inf. Theory*, vol. 46, no. 4, pp. 1204-1216, Jul. 2000.
- [7] J. Kim, S. Park, J. Kim, Y. Kim, H. Song, "Joint LDPC Codes for Multi-User Relay Channel," *Fourth Workshop on Network Coding, Theory and Applications (NetCod)*, pp. 1-6, Jan. 2008.
- [8] J. Li, J. Yuan, R. Malaney, and M. Xiao "Achievable rates and LDPC code design for a multi-source relaying system," *submitted to IEEE Transactions on Communications*.
- [9] S. Brink, G. Kramer, and A. Ashikhmin, "Design of Low-density parity-check codes for modulation and detection," *IEEE Trans. Commun.*, vol. 52, no. 4, pp. 670-678, Apr. 2004.
- [10] G. Liva and M. Chiani, "Protograph LDPC codes design based on EXIT analysis," *IEEE Global Telecommunications Conference (GLOBECOM)*, pp. 3250-3254, Nov. 2007.
- [11] E. Sharon, A. Ashikhmin, and S. Litsyn, "Analysis of low-density parity-check codes based on EXIT Functions," *IEEE Trans. Commun.*, vol. 54, no. 8, pp. 1407-1414, Aug. 2006.
- [12] "A fast and accurate degree distribution optimizer for LDPC code ensembles," Available Online: <http://lthcwww.epfl.ch/research/ldpcopt>.